nature biotechnology

Pairwise agonist scanning predicts cellular signaling responses to combinatorial stimuli

Manash S Chatterjee[1], Jeremy E Purvis[2], Lawrence F Brass[3] & Scott L Diamond[1,2]

Prediction of cellular response to multiple stimuli is central to evaluating patient-specific clinical status and to basic understanding of cell biology. Cross-talk between signaling pathways cannot be predicted by studying them in isolation and the combinatorial complexity of multiple agonists acting together prohibits an exhaustive exploration of the complete experimental space. Here we describe pairwise agonist scanning (PAS), a strategy that trains a neural network model based on measurements of cellular responses to individual and all pairwise combinations of input signals. We apply PAS to predict calcium signaling responses of human platelets in EDTA-treated plasma to six different agonists (ADP, convulxin, U46619, SFLLRN, AYPGKF and PGE_2) at three concentrations (0.1, 1 and 10 × EC_{50}). The model predicted responses to sequentially added agonists, to ternary combinations of agonists and to 45 different combinations of four to six agonists ($R = 0.88$). Furthermore, we use PAS to distinguish between the phenotypic responses of platelets from ten donors. Training neural networks with pairs of stimuli across the dose-response regime represents an efficient approach for predicting complex signal integration in a patient-specific disease milieu.

Because cells produce integrated responses to dose-dependent combinations of numerous external signals, efficient methods are needed to survey such high-dimensional systems. Primary human tissues such as blood, marrow or biopsies provided a limited number of cells, generally allowing only ~10^2 or fewer phenotypic tests. Evaluating the cellular response to pairs of stimuli offers a direct and rapid sampling of a response space that can be built-up into a higher level predictive tool through the use of neural networks. Such methods are needed to better phenotype platelets to predict cardiovascular risk. Platelets are cells that respond in a donor-specific manner to multiple signals *in vivo*, and their activation in response to thrombotic signals is central to the thrombotic risks and events surrounding 1.74 million heart attacks and strokes, 1.115 million angiograms and 0.652 million stent placements in the United States each year[1]. Moreover, platelets are ideal 'reduced' cellular systems for quantifying the effects of multiple signaling pathways because they are anucleate, easily obtained from donors and amenable to automated liquid handling.

During clotting, platelets experience diverse signaling cues simultaneously. Collagen activates glycoprotein VI (GPVI)-dependent tyrosine kinase signaling. ADP is released from dense granules to activate the G protein–coupled receptors P_2Y_1 and P_2Y_{12}. Thromboxane A_2 (TxA_2) is synthesized by platelet cyclooxygenase (COX)1 and binds thromboxane-prostanoid (TP) receptors. Tissue factor at the damaged vasculature leads to the production of thrombin, which cleaves the protease-activated receptors PAR1 and PAR4. These activating signals occur in the context of inhibitory signals from endothelial nitric oxide and prostacyclin (PGI_2). Platelets receive these signaling events simultaneously *in vivo*, and platelet signaling varies spatially and temporally in growing thrombi[2], but few experimental or computational tools are available for building a global understanding of how the platelet integrates multiple stimuli present at varying levels.

To predict cellular responses to multiple stimuli, we developed PAS (**Fig. 1**). This strategy involves selecting stimuli molecules based on prior knowledge (**Fig. 1a**), measuring cellular responses to all pairwise combinations of stimuli in a high-throughput manner (**Fig. 1b**), and then training a two-layer, nonlinear, autoregressive neural network with the cellular responses to exogenous inputs (**Fig. 1c**). Neural networks are remarkable in learning patterns of inputs and predicting outputs by optimizing intermediate connection weights, akin to a platelet's ability to respond to multiple thrombotic signals through coupled biochemical reactions. Motivated by the notion that a living cell is essentially a neural network whose connection weights have been selectively adjusted during evolution[3], we took a 'top-down' approach[4] to model platelet signaling. The application of neural networks for predicting dynamic cellular signaling is beneficial because neural networks are 'dense' modeling structures—meaning that they do not require detailed knowledge of the kinetic structure of a system. By comparison, an ordinary differential equation model of ADP-stimulated calcium mobilization through P_2Y_1 required almost 80 reactions and over 100 kinetic parameters to describe just this one single pathway[5]. We estimate that an ordinary differential equation model that describes the signaling mechanisms of the six agonists (**Fig. 1a**) in this study on a similar level of detail would require >500 parameters, many of which are currently unavailable.

[1]Institute for Medicine and Engineering, Department of Chemical and Biomolecular Engineering, University of Pennsylvania, Philadelphia, Pennsylvania, USA. [2]Institute for Medicine and Engineering, Genomics and Computational Biology, University of Pennsylvania, Philadelphia, Pennsylvania, USA. [3]Institute for Medicine and Engineering, Department of Medicine, University of Pennsylvania, Philadelphia, Pennsylvania, USA. Correspondence should be addressed to S.L.D. (sld@seas.upenn.edu).

Received 18 October 2009; accepted 6 May 2010; published online 20 June 2010; doi:10.1038/nbt.1642

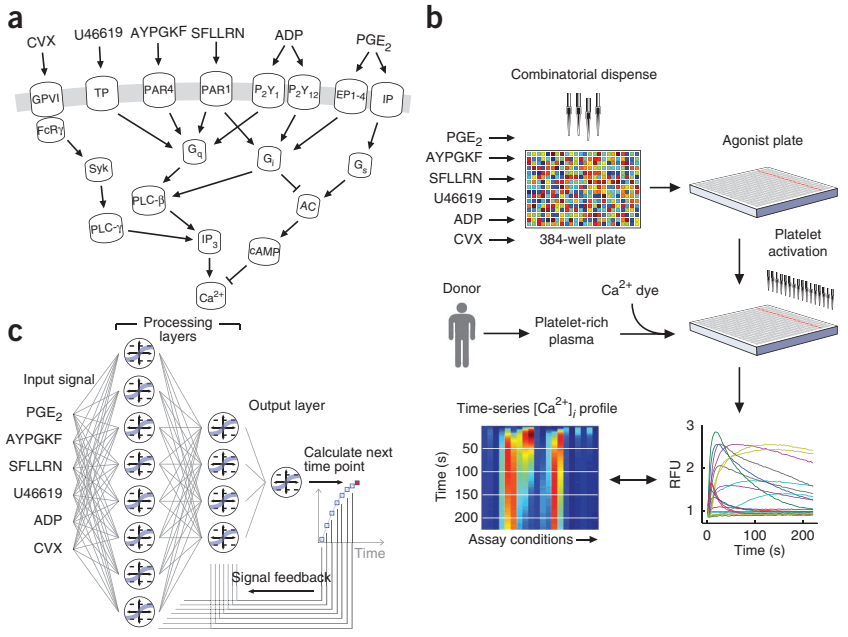

Figure 1 Experimental and computational methods to study platelet signaling. (**a**) Signaling pathways in platelets converge on intracellular calcium release. (**b**) High-throughput experimental procedure. An agonist plate containing combinatorial agonist combinations and a platelet plate containing dye-loaded platelets were separately assembled. Agonists were dispensed onto platelet suspensions and fluorescence changes were measured to quantify platelet calcium concentrations $[Ca^{2+}]_i$. $[Ca^{2+}]_i$ transients can be represented as overlapping plots (lower right) or parallel heat maps (lower left). RFU, relative fluorescent units. (**c**) Dynamic neural network used to train platelet response to combinatorial agonist activation. A constant sequence of input signals (agonist concentrations) is introduced to the two-layer, 12-node network at each time point. Processing layers integrate input values with feedback signals to predict $[Ca^{2+}]_i$ at the next time point.

We selected six major agonists of human platelets—convulxin (CVX; GPVI activator), ADP, the thromboxane analog U46619, PAR1 agonist peptide (SFLLRN), PAR4 agonist peptide (AYPGKF) and prostaglandin E2 (PGE_2) (activator of the prostacyclin receptor IP and the E series prostanoid receptors EP 1-4). These agonists activate platelet signaling pathways that converge on the release of intracellular calcium (Ca^{2+}) (**Fig. 1a**), which we measured using a fluorescent calcium dye. Calcium mobilization is critical to physiologically important platelet responses needed for aggregation and clotting, including granule release, exposure of phosphatidylserine, actin polymerization, shape change and integrin activation[6]. To determine appropriate dynamic ranges and the effective concentration for half-maximum response (EC_{50}) values for the six agonists, we first tested each compound individually to determine dose-response relationships (**Supplementary Fig. 1**). The inhibitory response of PGE_2 was studied by concomitantly stimulating the platelet with 60 μM SFLLRN.

To eliminate the sensitivity of cells to confounding autocrine effects of soluble mediators that are dependent on platelet concentrations and transport processes, we conducted all experiments in 5 mM EDTA, which chelates extracellular calcium. The removal of external calcium does not affect the ability of the studied receptors to signal, as no appreciable difference in EC_{50}s were noted with or without external calcium (**Supplementary Fig. 1a**,**b**). Although this experimental design does not capture the contribution of store-operated calcium entry, it offers several operational advantages by (i) lowering background fluorescence without extensive platelet washing, (ii) preventing thrombin production, (iii) inhibiting granule release[7,8] as well as TxA_2 formation[9] and (iv) inhibiting integrin-mediated signaling downstream of Ca^{2+} release[10]. The operational advantages of using EDTA, however, prevent prediction of important physiologic phenomena like granule release, integrin activation and outside-in signaling.

To test whether the intracellular Ca^{2+} signal detected was being influenced by endogenously released agonists, we studied the effects of 2 units/ml apyrase (which hydrolyzes released ADP) or 15 μM indomethacin (which inhibits production of TxA_2). Both of these inhibitors had no effect on individual responses (**Supplementary Fig. 2** and **Supplementary Tables 1** and **2**), suggesting that endogenous autocrine activators have no effect on the Ca^{2+} signal. This confirms that the resulting traces of Ca^{2+} are directly dependent only on receptor-mediated release from intracellular stores.

We applied the PAS method by first measuring platelet responses to all 135 pairwise combinations of low ($0.1 \times EC_{50}$), moderate ($1 \times EC_{50}$) and high ($10 \times EC_{50}$) agonist concentrations (**Fig. 2a**). Then, we trained a neural network model on 154 time-course traces (135 pairwise responses, 18 single-agonist responses, 1 null control response). We defined a pairwise agonist synergy score (S_{ij}) to be the scaled difference between the integrated transient (area under the curve) for the combined response and the integrated area for the individual responses (**Fig. 2b**) ($S_{ij} > 0$, synergism; $S_{ij} = 0$, additivity; $S_{ij} < 0$, antagonism). The trained network accurately reproduced the time-course behavior ($R = 0.968$ for correlation between time points) and the pairwise agonist synergy ($R = 0.884$) for correlation between S_{ij} scores (**Fig. 2a**,**b** and **Supplementary Fig. 3**).

As an initial test of the trained network, we predicted the response of platelets to all 64 ternary combinations of the agonists ADP, SFLLRN and CVX at 0, 0.1, 1 and $10 \times EC_{50}$ concentrations and compared the predictions to experimentally measured responses (**Fig. 3a**). A CVX response requires GPVI multimerization[11] and is characterized by a slow rise to a large peak signal followed by a slow decline. G_q-coupled responses (ADP or SFLLRN) produce rapid bursts that are quickly brought down to baseline. Increasing CVX for a fixed ADP level resulted in a steady increase in Ca^{2+} on longer timescales. In contrast, increasing ADP for a fixed CVX level bolstered early Ca^{2+} release. A moderate dose of both ADP and CVX (for 0 and low SFLLRN) produced a response that almost instantaneously plateaued at a steady level above baseline. Both the time-course behavior ($R = 0.844$) and ternary agonist synergy scores ($R = 0.881$) (**Supplementary Fig. 4**) were accurately reproduced for the 27 unique ternary conditions in this experiment that were not present in the training set.

To fully test and utilize the predictive power of the neural network, we made *in silico* time-course and synergy predictions for the complete six-dimensional agonist space consisting of 4,077 unique agonist combinations of two to six agonists at 0.1, 1 or $10 \times EC_{50}$ concentrations (**Supplementary Fig. 5**). Based on these predictions, we selected 45 combinations of four, five or six agonists that displayed a range of predicted synergy scores from synergy to strong

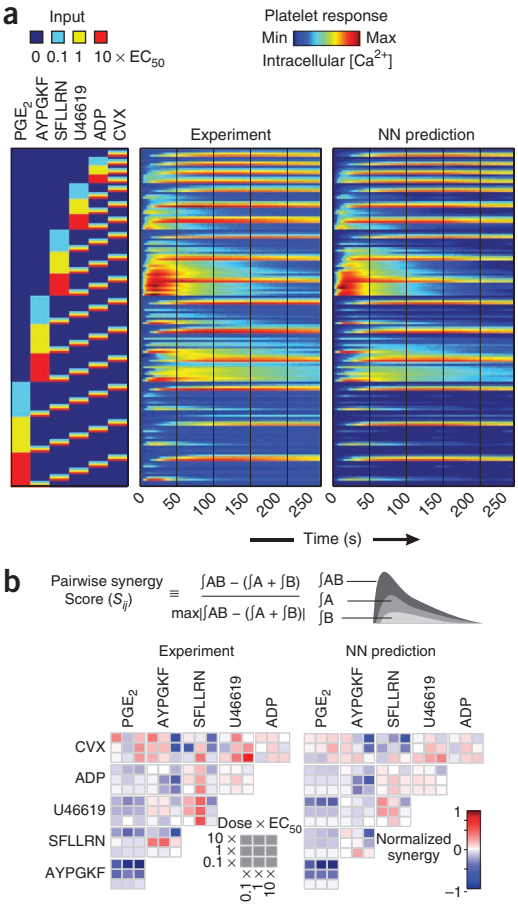

Figure 2 PAS. (**a**) All 154 binary combinations of the agonists CVX, ADP, U46619, SFLLRN, AYPGKF and PGE_2 at concentrations of 0, 0.1, 1 and 10 × EC_{50} were combined on the same plate (in replicates of 2) and the dynamic response of the platelet to each combination was recorded. The neural network model was trained on this dataset. (**b**) Pairwise agonist synergy scores, which reflect the gain or loss in calcium response due to agonist cross-talk, were calculated for both experimental and predicted time-course traces. EC_{50}: PGE_2, 24.6 μM; AYPGKF, 112 μM; SFLLRN, 15.2 μM; U46619, 1.19 μM; ADP, 1.17 μM; CVX, 0.00534 μM.

antagonism and tested them experimentally in addition to no agonist and 18 single-agonist controls (**Fig. 3b**). To prevent any bias in the selection, we picked conditions that had maximal dissimilarity in the types and concentrations of agonists. We found strong agreement between both predicted and measured transient shapes ($R = 0.845$) (**Fig. 3b** and **Supplementary Fig. 6a**), as well as between predicted and measured S_{ij} scores ($R = 0.883$, slope = 1.08) (**Fig. 3c**). For comparison, the full distribution of synergy predictions for all 4,077 agonist combinations is shown as a vertical heat map in **Figure 3c**. To investigate whether smaller subsets of inputs, such as dominant pairs, could account for the network's predictive accuracy, we retrained the neural network on different subsets of inputs. This typically, and almost always, reduced predictive accuracy (**Supplementary Fig. 6b**), suggesting that the neural network does not exclusively rely on smaller subsets of input.

Conditions containing high levels of all agonists showed especially low synergy due to saturation of Ca^{2+} release. The highest synergy was observed for agonist combinations that contained high levels of the thromboxane analog U46619 with no PGE_2 present (**Fig. 3c**, orange bar). Given that only 8 of 45 conditions had maximal U46619/PGE_2 ratio, this ordering of the top three conditions was highly significant ($P < 0.004$), considering there are 14,190 possible ways to order the first three conditions of which only 56 combinations would contain high U46619 and low PGE_2. Thus, the neural network model trained on pairwise data facilitated discovery of a high-dimensional synergy that occurs at a high U46619/PGE_2 ratio (at low levels of ADP, SFLLRN and submaximal levels of AYPGKF) consistent with the known cardiovascular risks of COX2 inhibitors that prevent endothelial production of PGI_2 without affecting platelet production of thromboxane[12]. This points to a 'high-dimensional' COX2 inhibition risk of high concentrations of thromboxane, in the absence of PGI_2, potentiating the effects of other agonists.

We also explored the effect of adding the agonists ADP, SFLLRN and CVX in various sequential combinations (**Fig. 3d**). Several notable behaviors were accurately predicted by the neural network model despite the network being trained on purely synchronous interactions. For instance, the temporal sequence ADP-SFLLRN-CVX (**Fig. 3d**, panel 1) produced three distinct Ca^{2+} bursts, whereas the ADP response was completely abolished in the sequence SFLLRN-ADP-CVX (**Fig. 3d**, panel 3). This behavior points to mechanisms of cross-downregulation of ADP signaling by component(s) of the PAR1 cascade. (See **Supplementary Discussion** and **Supplementary Fig. 7** for tests with thrombin compared to SFLLRN+AYPGKF).

To investigate the reproducibility of the PAS procedure and to investigate the potential for using it to stratify individuals' platelet responses, we performed PAS twice in a 2-week period for ten healthy male donors (**Fig. 4**). The 135 conditions containing pairs of agonists in a single PAS experiment make up the synergy map for each donor experiment (**Supplementary Fig. 8**) and individual columns of the synergy matrix (**Fig. 4**). The standard errors in synergy scores across all 135 conditions were uncorrelated with the magnitude of synergy and are measures of the experimental uncertainty and day-to-day fluctuations in mean synergy values at these conditions. The mean uncertainty for a representative donor (donor A) was ±0.0523 for S_{ij} ranging from −1 to 1 (uncertainties across all 135 conditions are shown in **Supplementary Fig. 9**). The mean standard error in synergy scores for all ten donors ranged from ±0.0347 to ±0.0627 (**Supplementary Table 3**).

We generated a hierarchical cluster tree using the Euclidean distances between donor experiments. Seven of the ten donor pair vectors (donor pairs D, C, A, H, E, F and I) self-clustered, demonstrating that despite variation between samples from the same donor, pronounced inter-donor variations allow us to distinguish donors. This pattern of clustering was found to be highly significant ($P < 8 \times 10^{-7}$) by randomizing observed donor synergies (**Supplementary Fig. 10**). The observed pattern of self-clustering was platelet signaling dependent (and not related to donor plasma), as the PAS scans of an individual donor's platelets with autologous or heterologous plasma self-clustered (**Supplementary Fig. 11**). In general, across all conditions and donors, the highest probability of pairwise synergy was observed when moderate doses of both agonists were used. Low doses of both agonists produced additive responses, whereas high doses of both agonists skewed synergy distributions toward antagonism (**Supplementary Fig. 12**).

Donors separated into at least two major subgroups with the cluster of donor experiments D1, D2, J2, C1, C2, B1 and B2 characterized by relative lack of synergy in comparison to other experiments. The cluster of experiments A1, A2, H1, H2, J1, E1, E2, F1, F2, G1, I1, I2 and G2 had marked synergy between moderate doses of SFLLRN and all doses of U46619 or ADP, as

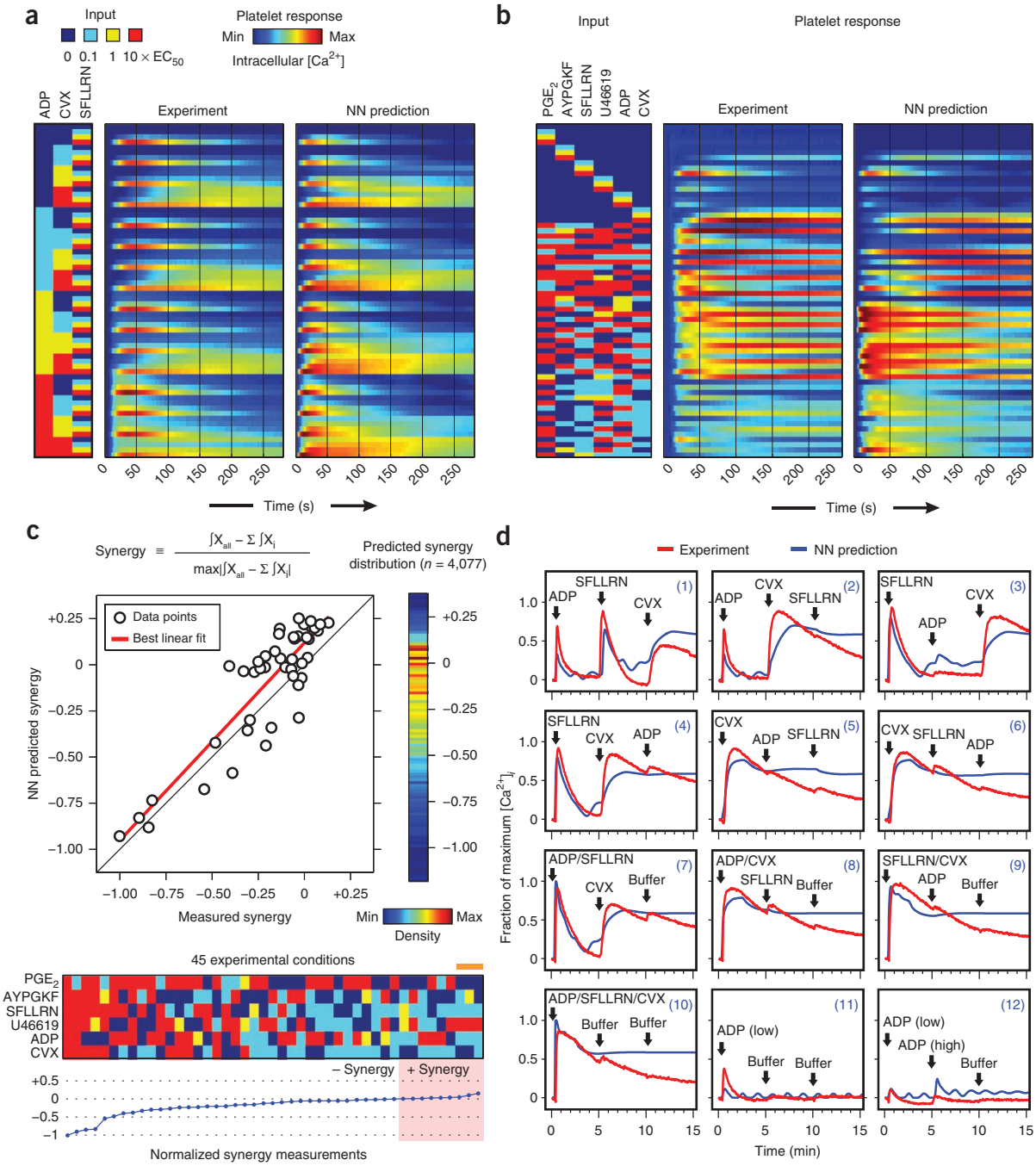

Figure 3 Neural network model reveals the global platelet response to all agonist combinations. (**a**) Measurement and prediction of the platelet response to all 64 ternary combinations of ADP, SFLLRN and CVX at 0, 0.1, 1 and 10 × EC_{50}. The neural network model was trained only on pairwise interactions but successfully predicted ternary interactions. (**b**) Measurement and prediction of the platelet response to 45 predictions in the full combinatorial agonist space. (**c**) Predicted versus measured synergy scores for the 45 conditions in **b** (upper left). Distribution of synergy scores for all 4,077 possible experimental conditions (upper right). Experimental conditions for the 45 sampled combinations of agonists, arranged in order of increasing synergy (bottom). The orange bar denotes the three most highly synergistic conditions, which all contained high U46619, no PGE_2 and low levels of other agonists. (**d**) Measured and predicted platelet responses to sequential additions of ADP, SFLLRN and CVX.

well as marked synergy for moderate U46619 and high CVX. All donors showed some synergism between low and moderate doses of SFLLRN and U46619. We also typically observed synergy between AYPGKF and U46619. Moreover, synergistic or additive interactions were noted also between low and moderate doses of SFLLRN and AYPGKF. These results suggested a mechanism of synergy between thrombin and thromboxane. To test this, binary synergy maps of the physiological agonist thrombin and U46619 were constructed for donors A and E (**Supplementary Fig. 13**) over seven doses spanning the active concentration ranges. To our knowledge, this is the first report of conserved synergy between thrombin and thromboxane mimetics.

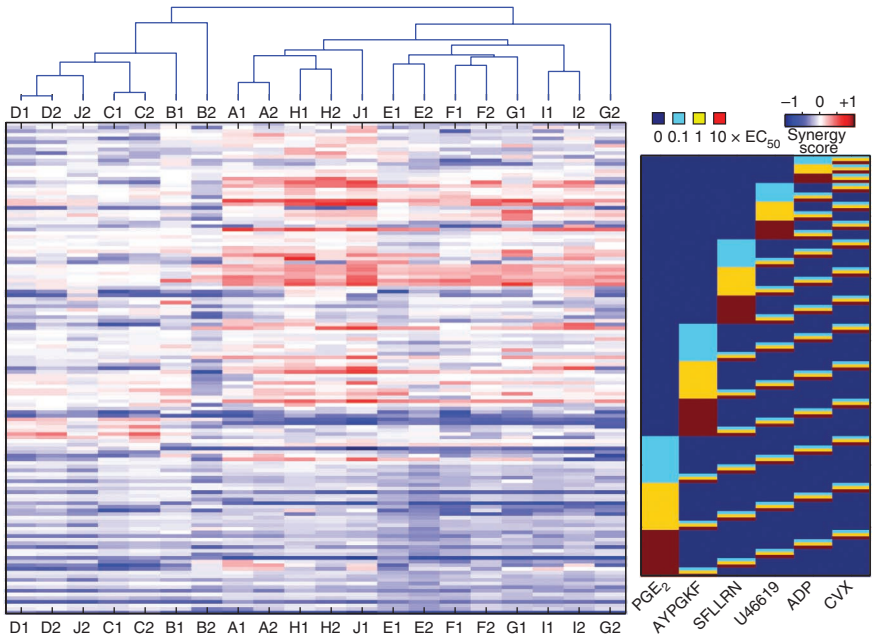

Figure 4 Donor-specific synergy maps. Ten healthy donors were phenotyped for platelet calcium response to all pairwise agonist combinations. Repeat experiments were conducted within 2 weeks. Donors (ages, 22–30 years) spanned several ethnic groups (three Western Europeans, two Asians, two Indians, one Caribbean, one African American and one African). The magnitudes of synergy in each of the 20 donor-specific synergy maps were arranged as columns of the synergy matrix. These vectors were clustered according to similarity using a distance-based clustering algorithm.

Studying the combinatorial effects of pairs of agonists in low, moderate and high concentrations allowed a rapid, donor-specific phenotypic scan that was predictive of responses to multiple agonists. Importantly, a single 384-well plate of data was sufficient to train a neural network model (**Fig. 2**) capable of making accurate predictions of the global six-dimensional agonist reaction space (**Fig. 3**), which is difficult to probe experimentally but fundamental to the processes of thrombosis. Synergies between platelet agonists are dependent not just on agonist pairs and doses, but also vary from donor to donor (**Fig. 4**). In contrast to PAS, current measurements of platelet phenotype can only coarsely stratify healthy donors. For instance, platelet aggregometry has been used[13] to classify 359 individuals as "hypo- or hyper-" reactive to platelet agonists; and flow cytometry was used[14] to classify 26 individuals as high, medium or low responders. Previous studies have reported synergistic aggregation responses of platelets to combinations of multiple agonists[15–17]. Such unique patterns of synergisms could be used to distinguish donors and be correlated with certain risk factors. Clinically, we anticipate that PAS profiles will depend on variables such as ancestry, age, sex, pharmacology and cardiovascular state—all of which require further testing—although linking genotype (1,327 single nucleotide polymorphisms) to phenotype (flow cytometric measurement of P-selectin exposure and fibrinogen binding) in 500 individuals[18] demonstrated only weak association probabilities.

The PAS approach works because individual and binary interactions dominate, and they are sampled across the full dose range of inputs. We expect the method to break down when ternary interactions in excess of summing binary interactions become strong. We show that the residual ternary synergy ($\Delta(ABC) = S_{ABC} - S_{AB} - S_{BC} - S_{AC}$) was ~0 in each of 27 responses of platelets to different ternary combinations of CVX, ADP and SFLLRN and was minimized in the neural network model training (**Supplementary Fig. 14** and **Supplementary Discussion**). In general, knowledge of pairwise interactions alone cannot be expected to predict response to several simultaneously present stimuli (>2). However, certain characteristics of platelets and the conditions under which they were studied made such an approach feasible in this instance. These include (i) the relative abundance of binary interactions in signaling systems with minimized ternary interactions (**Supplementary Fig. 14**)[19]; (ii) the efficient utilization of system history (**Supplementary Fig. 15**); (iii) the dense sampling of interactions across a full dose-response range; (iv) known intracellular wiring that rapidly converges on Ca^{2+}, without the possibility of higher order effects from genetic regulation or other interactions on long time scales; and (v) choice of well-characterized extracellular ligands and careful design to avoid autocatalytic feedback.

Further, application of PAS to stimuli including epinephrine, soluble CD40L, serotonin and nitric oxide would map a major portion of the entire platelet response space. The use of PAS with orthogonal pharmacological agents (indomethacin, P_2Y_{12} inhibitors, selective PAR antagonists, quanylate cyclase or adenylate cyclase inhibitors) would allow further assessment of individual clinical risk or sensitivity to therapy. The PAS method demonstrates that sampling all dual orthogonal 'axes' (every agonist pair) can successfully predict the dynamic responses and cross-talk of a system receiving complex combinations of inputs.

METHODS

Methods and any associated references are available in the online version of the paper at http://www.nature.com/naturebiotechnology/.

Note: Supplementary information is available on the Nature Biotechnology website.

ACKNOWLEDGMENTS

The authors thank H. Li for suggesting the permutation test to evaluate the significance of donor clustering. This work was supported by the US National Institutes of Health R01-HL-56621 (S.L.D.), R33-HL-87317 (S.L.D. and L.F.B.) and T32-HG000046 (J.E.P.).

AUTHOR CONTRIBUTIONS

M.S.C. designed and performed all experiments. J.E.P. constructed neural network models of platelet activation. M.S.C. wrote the paper with contributions from all authors. L.F.B. advised on experimental conditions, and S.L.D. conceived the study.

COMPETING FINANCIAL INTERESTS

The authors declare no competing financial interests.

Published online at http://www.nature.com/naturebiotechnology/.
Reprints and permissions information is available online at http://npg.nature.com/reprintsandpermissions/.

1. Lloyd-Jones, D. *et al.* Heart disease and stroke statistics–2009 update: a report from the American Heart Association Statistics Committee and Stroke Statistics Subcommittee. *Circulation* **119**, e21–e181 (2009).
2. Furie, B. & Furie, B.C. *In vivo* thrombus formation. *J. Thromb. Haemost.* **5**, 12–17 (2007).
3. Bray, D. Protein molecules as computational elements in living cells. *Nature* **376**, 307–312 (1995).

4. Bray, D. Molecular networks: the top-down view. *Science* **301**, 1864–1865 (2003).
5. Purvis, J.E., Chatterjee, M.S., Brass, L.F. & Diamond, S.L. A molecular signaling model of platelet phosphoinositide and calcium regulation during homeostasis and P2Y1 activation. *Blood* **112**, 4069–4079 (2008).
6. Siess, W. Molecular mechanisms of platelet activation. *Physiol. Rev.* **69**, 58–178 (1989).
7. Bohne, A., Fukami, M.H. & Holmsen, H. EDTA inhibits collagen-induced ATP plus ADP secretion and tyrosine phosphorylation in platelets independently of Mg2+ chelation and decrease in pH. *Platelets* **13**, 437–442 (2002).
8. Lages, B. & Harvey, J.W. Heterogeneous defects of platelet secretion and responses to weak agonists in patients with bleeding disorders. *Br. J. Haematol.* **68**, 53–62 (1988).
9. Cho, M.J. *et al.* The roles of alpha IIbbeta 3-mediated outside-in signal transduction, thromboxane A2, and adenosine diphosphate in collagen-induced platelet aggregation. *Blood* **101**, 2646–2651 (2003).
10. Brass, L.F., Shattil, S.J., Kunicki, T.J. & Bennett, J.S. Effect of calcium on the stability of the platelet membrane glycoprotein IIb-IIIa complex. *J. Biol. Chem.* **260**, 7875–7881 (1985).
11. Polgar, J. *et al.* Platelet activation and signal transduction by convulxin, a C-type lectin from *Crotalus durissus terrificus* (tropical rattlesnake) venom via the p62/GPVI collagen receptor. *J. Biol. Chem.* **272**, 13576–13583 (1997).
12. Mukherjee, D., Nissen, S.E. & Topol, E.J. Risk of cardiovascular events associated with selective COX-2 inhibitors. *JAMA* **286**, 954–959 (2001).
13. Yee, D.L., Sun, C.W., Bergeron, A.L., Dong, J.-f. & Bray, P.F. Aggregometry detects platelet hyperreactivity in healthy individuals. *Blood* **106**, 2723–2729 (2005).
14. Panzer, S., Höcker, L. & Koren, D. Agonists-induced platelet activation varies considerably in healthy male individuals: studies by flow cytometry. *Ann. Hematol.* **85**, 121–125 (2006).
15. Packham, M.A., Guccione, M.A., Chang, P.L. & Mustard, J.F. Platelet-aggregation and release-effects of low concentrations of thrombin or collagen. *Am. J. Physiol.* **225**, 38–47 (1973).
16. Grant, J.A. & Scrutton, M.C. Positive interaction between agonists in the aggregation response of human-blood platelets-interaction between adp, adrenaline and vasopressin. *Br. J. Haematol.* **44**, 109–125 (1980).
17. Hallam, T.J., Scrutton, M.C. & Wallis, R.B. Synergistic responses and receptor occupancy in rabbit-blood platelets. *Thromb. Res.* **27**, 435–445 (1982).
18. Jones, C.I. *et al.* A functional genomics approach reveals novel quantitative trait loci associated with platelet signaling pathways. *Blood* **114**, 1405–1416 (2009).
19. Hsueh, R.C. *et al.* Deciphering signaling outcomes from a system of complex networks. *Sci. Signal.* **2**, ra22 (2009).

ONLINE METHODS

Materials. PAR1-agonist peptide SFLLRN (thrombin receptor agonist peptide, TRAP) and the PAR4-agonist peptide AYPGKF were obtained from Bachem. Convulxin (CVX) was obtained from Centerchem. Thrombin and GGACK were obtained from Haematologic Technologies. Clear, flat-bottom, black 384-well plates were obtained from Corning. ADP, U46619, PGE2, EDTA, HEPES, the fibrin polymerization inhibitor Gly-Pro-Arg-Pro (GPRP), NaCl, NaOH, apyrase, indomethacin and sodium citrate were all from Sigma. Fluo-4 NW Calcium assay kits were obtained from Invitrogen. The buffer used for all dilutions was HEPES buffered saline (HBS, sterile filtered 20 mM HEPES and 140 mM NaCl in deionized water adjusted to pH 7.4 with NaOH).

Platelet preparation. Whole blood was drawn from healthy male volunteers according to the University of Pennsylvania Institutional Review Board guidelines, into citrate anticoagulant (1 part sodium citrate to 9 parts blood). All donors affirmed to not taking any medications for the past 10 d and not consuming alcohol for the past 3 d before phlebotomy. After centrifugation at 120*g* for 12 min to obtain platelet-rich plasma, 2 ml of platelet-rich plasma was incubated with each vial of Fluo4-NW dye mixture reconstituted into 8 ml of buffer for 30 min.

High-throughput experimentation. An 'agonist plate' containing varying combinatorial concentrations of platelet agonists was prepared on a PerkinElmer Janus (PerkinElmer Life and Analytical Sciences) using 10× stock solutions of ADP, CVX, SFLLRN, AYPGKF and U46619. A separate 'platelet plate' containing dye-loaded platelets was prepared on a PerkinElmer Evolution. Final platelet rich plasma (PRP) concentrations were 12% by volume (6 µl/well) after agonist addition, and 5 mM EDTA was included in every well. Agonists (10 µl/well) were dispensed after a 20-s baseline read from columns of the 'agonist plate' onto the corresponding columns of the 'platelet plate' on a Molecular Devices FlexStation III. Fluo4 fluorescence was measured at excitation 485 nm and emission 535 nm for 4 min in every column of the plate. The fluorescence $F(t)$ was scaled to the mean baseline value for each well $F_0(t)$ and relative calcium concentrations were quantified as $F(t)/F_0(t)$. An entire 384-well plate was read in ~90 min.

Agonist selection. The number of agonists tested in a PAS experiment is limited to six by the need of testing all the 154 conditions in duplicate in a single 384-well plate. Agonists were chosen to be representative of physiological signaling cascades. Convulxin is a selective GPVI activator[11] and under static conditions this receptor is the predominant determinant of collagen-induced signal strength[20] . In contrast, the soluble monomeric form of collagen interacts only with $\alpha_2\beta_1$, which regulates platelet adhesion but has little direct effect in mediating signaling[21,22]. 'Horm' collagen preparations are insoluble, making them poorly suited for automated liquid handling. Although ADP stimulates both P_2Y_1 and P_2Y_{12}, the latter receptor has a minor effect on calcium mobilization[23], allowing us to use the physiological agonist ADP instead of specific P_2Y_1 ligands. Thrombin signals through two separate G_q-coupled receptors PAR1 and PAR4, both of which produce temporally separate calcium signals[24,25]. This prompted us to use selective PAR agonist peptides (SFLLRN and AYPGKF) to distinguish the separate signal contribution of both these receptor pathways. Moreover, thrombin stimulation of unwashed PRP requires inhibition of fibrin and coagulation factor Xa (FXa) formation (**Supplementary Fig. 13**). Washing or gel-filtering platelets are processing steps that decrease throughput in a large-scale experiment and often cause residual platelet activation in the absence of PGE_2 or other PGI_2 analogs. The use of a short-lived prostaglandin like PGI_2 (ref. 26) is unsuitable for assembly of agonist plates (requiring ~120 min) and plate reading (requiring ~90 min). In contrast, prostaglandins of the E series are chemically stable, prompting us to use PGE_2 as an agonist causing elevation in intracellular cAMP. Similarly, for reasons of stability during the course of the experiment, the thromboxane analog U46619 was used instead of its physiological equivalent TxA_2 (ref. 27).

Definition of synergy score. To quantify cross-talk between agonist combinations, we defined the 'synergy score' as the difference between the observed and the predicted additive response. For ease of visualization, this difference was scaled to the maximum synergy score observed in an experiment (or simulation), giving a metric that ranges from −1 (antagonism) to +1 (positive synergy). A similar synergy metric was previously defined as the ratio of the observed and the predicted additive response to demonstrate synergistic calcium signaling between C5a and UDP in RAW264.7 cells and bone marrow–derived macrophages[28]. The use of a ratio rather than a difference is prone to numerical errors for small values of the predicted additive response.

Neural network model construction, training and simulation. Neural network modeling and analysis was performed using the Neural Network Toolbox for MATLAB (The MathWorks). Training data consisted of (i) the dynamic inputs, which represent the combination of agonist concentrations present at each time point for a particular experiment (because the concentration of agonists remains essentially constant throughout each experiment, these values were generally a constant vector of concentration values repeated at 1-s intervals) and (ii) the dynamic outputs, which represent the experimentally measured calcium concentrations, also interpolated at 1-s intervals. To normalize the input data, agonist concentrations of 0, 0.1, 1 and 10 × EC_{50} were mapped to the values (−1, −0.333, +0.333, +1) before introducing them to the network, so as to fall within the working range of the hyperbolic tangent sigmoid transfer function, which was used for all processing nodes. Output values (fluorescence measurements) were normalized between −1 and +1, so that the basal concentration of calcium at $t = 0$ was defined to be 0. After training all 420 possible one- and two-layer neural networks with between 1 and 20 nodes in each processing, or 'hidden', layer and testing each network for accuracy, a final neural network topology with a six-node input layer (representing the six agonists), two processing layers (eight nodes/four nodes) and a single-node output layer (representing the intracellular calcium concentration)[29] was most optimal (best predicted the 'net' output response $[Ca^{2+}]_I$ for a given multivariate input using the fewest neurons) and thus selected to predict successive time points from all 154 Ca^{2+} release curves gathered experimentally (**Fig. 2**). For the sake of simplicity and because we already obtain reasonably accurate time series predictions of $[Ca^{2+}]_i$, more processing layers or >20 neurons in each layer were not tested. From a purely biological perspective, the model architecture is arbitrary and no particular meaning should be inferred from the narrowing of eight nodes in the first layer to four nodes in the second processing layer. Moreover, this neural network model (**Fig. 1c**) does not correspond to an actual signaling network (**Fig. 1a**) but does provide a highly efficient framework for use as an independent signaling module in multiscale models of thrombosis under flow. From a mathematical perspective, this architecture represents a multivariate regression to obtain optimal good fits of high-dimensional data and allow extrapolation onto experimentally unexplored spaces.

NARX (nonlinear autoregressive network with exogenous inputs) models are recurrent dynamic networks with feedback connections enclosing multiple layers of the network and are well-suited for predicting time series data[30] because they process inputs sequentially, that is, at successive time points. Calcium outputs before the current instant were fed back to hidden layers using a delay line spanning 128 s. Initial states of the delay line were set to 0, corresponding to the steady state of the platelet before agonist stimulation. Such a structure allows the network output to progress over time, using the 'memory' of the previous 128 s in calculating the current output. Training was performed using Levenberg-Marquardt back-propagation until the performance of the model (mean squared error between the simulated and experimentally measured PAS responses) did not become better than $>1 \times 10^{-5}$. During training, the pairwise agonist data (154 time-course traces) was divided into training, validation and testing vectors. Validation and testing vectors were each generated by randomly selecting 23 (15%) of the 154 pairwise time-course traces. The training vectors were used to directly optimize network edge weights and bias values to match the target output. The validation set was used to ensure that there is no overfitting in the final result. The test vectors provide an independent measure of how well the network can be expected to perform on data not used to train it

Mathematically, the output y at an instant t, for an input vector $\bar{I}$ of the concentrations of the six inputs species can be compactly described by

$$y(t) = \underbrace{f\left(\overline{L3}_{(1\times4)} \times \underbrace{f\left(\overline{\overline{H2}}_{(4\times8)} \times \overline{y_h}_{(8\times1)} + \overline{L2}_{(4\times8)} \times \underbrace{f\left(\overline{\overline{H1}}_{(8\times8)} \times \overline{y_h}_{(8\times1)} + \overline{\overline{IW}}_{(8\times6)} \times \bar{I}_{(6\times1)} + \overline{b1}_{(8\times1)}\right)}_{(8\times1)}\right)}_{(4\times1)} + \overline{b2}_{(4\times1)}\right)}_{(1\times1)} + \overline{b3}_{(1\times1)}$$

where $\overline{\overline{IW}}$ is the matrix of input weights, $\overline{\overline{L2}}$ and $\overline{\overline{L3}}$ are the weight matrices that operate on the 'inputs' coming from the first and second processing layers respectively. $\overline{\overline{H1}}$ and $\overline{\overline{H2}}$ are matrices that contain history coefficients that weigh the history vector y_h (containing the output of the system 1, 2, 4, 8, 16, 32, 64 and 128 s prior to the current instant). $\overline{b1}$, $\overline{b2}$ and $\overline{b3}$ are bias vectors that add constant biases to each weighted input and weighted histories to produce the 'net input' to each transfer function. f is the hyperbolic tangent function that operates on a vector of 'net inputs' to yield the corresponding transformed output. Numbers in parentheses show the sizes of relevant matrices or vectors. The NARX model presented here represents a nonlinear regression model with input stimuli and system history. The use of simple 1st and 2nd order polynomial terms (with lower number of optimizable parameters) did not produce acceptable fits (not shown), necessitating the use of the NARX architecture. A 3rd order polynomial was not attempted since it requires 316 fitting parameters, far exceeding the number of parameters in the neural network model.

It should be noted that each trained neural network model produces a deterministic prediction of platelet activation. Experimental variations are inherent in replicates of donor-specific training data (**Supplementary Fig. 9**), and the tightness of the measured mean will determine the predictive quality of such a donor-specific neural network model.

The fold-expression kinetics of nine 'top-ranked' genes involved in the sustained migration of keratinocytes after hepatocyte growth factor (HGF) treatment has been described by means of a continuous-time recurrent neural network, and the neural network weights were used to define the modulation and control elements of the response[31]. Also, previous studies have used partial least-squares regression analysis (PLSR) to understand the interplay of molecular mechanisms during signaling[32,33]. PLSR measures multiple intermediate signaling molecules at various time points for a relatively small number of inputs, and identifies principal components that capture the phenotype of the system. In comparison, the PAS approach offers less mechanistic dissection but provides rapid (a 2-h experiment) and efficient prediction of dynamic input-output relationships at numerous (~10^2) physiologically relevant conditions.

20. Nieswandt, B. & Watson, S.P. Platelet-collagen interaction: is GPVI the central receptor? *Blood* **102**, 449–461 (2003).
21. Knight, C.G. *et al.* Collagen-platelet interaction: Gly-Pro-Hyp is uniquely specific for platelet Gp VI and mediates platelet activation by collagen. *Cardiovasc. Res.* **41**, 450–457 (1999).
22. Hers, I. *et al.* Evidence against a direct role of the integrin alpha2beta1 in collagen-induced tyrosine phosphorylation in human platelets. *Eur. J. Biochem.* **267**, 2088–2097 (2000).
23. Foster, C.J. *et al.* Molecular identification and characterization of the platelet ADP receptor targeted by thienopyridine antithrombotic drugs. *J. Clin. Invest.* **107**, 1591–1598 (2001).
24. Covic, L., Gresser, A.L. & Kuliopulos, A. Biphasic kinetics of activation and signaling for PAR1 and PAR4 thrombin receptors in platelets. *Biochemistry* **39**, 5458–5467 (2000).
25. Shapiro, M.J., Weiss, E.J., Faruqi, T.R. & Coughlin, S.R. Protease-activated receptors 1 and 4 are shutoff with distinct kinetics after activation by thrombin. *J. Biol. Chem.* **275**, 25216–25221 (2000).
26. Cho, M.J. & Allen, M.A. Chemical stability of prostacyclin (PGI_2) in aqueous-solutions. *Prostaglandins* **15**, 943–954 (1978).
27. Coleman, R.A., Humphrey, P.P.A., Kennedy, I., Levy, G.P. & Lumley, P. Comparison of the actions of U-46619, a prostaglandin H2-analogue, with those of prostaglandin-H2 and thromboxane-A2 on some isolated smooth-muscle preparations. *Br. J. Pharmacol.* **73**, 773–778 (1981).
28. Roach, T.I.A. *et al.* Signaling and crosstalk by C5a and UDP in macrophages selectively use PLCbeta 3 to regulate intracellular free calcium. *J. Biol. Chem.* **283**, 17351–17361 (2008).
29. Jain, L.C. & Medsker, L.R. *Recurrent Neural Networks: Design and Applications* (CRC Press, 1999).
30. Eugen, D. The use of NARX neural networks to predict chaotic time series. *WSEAS Trans. Comp. Res.* **3**, 182–191 (2008).
31. Busch, H. *et al.* Gene network dynamics controlling keratinocyte migration. *Mol. Syst. Biol.* **4**, 199 (2008).
32. Janes, K.A. *et al.* Systems model of signaling identifies a molecular basis set for cytokine-induced apoptosis. *Science* **310**, 1646–1653 (2005).
33. Kemp, M.L., Wille, L., Lewis, C.L., Nicholson, L.B. & Lauffenburger, D.A. Quantitative network signal combinations downstream of TCR activation can predict IL-2 production response. *J. Immunol.* **178**, 4984–4992 (2007).

doi:10.1038/nbt.1642